J. Biochem. 2009;145(2)217–227
doi:10.1093/jb/mvn160

Inhibition of the 20S Proteosome by a Protein Proteinase Inhibitor: Evidence That a Natural Serine Proteinase Inhibitor Can Inhibit a Threonine Proteinase

Kimihiko Yabe and Takehiko Koide*

Department of Life Science, Graduate School of Life Science, University of Hyogo, Harima Science Garden City, Hyogo 678-1297, Japan

Received November 1, 2008; accepted November 19, 2008; published online December 2, 2008

The 20S proteasome (20S) is an intracellular threonine proteinase (Mr 750,000) that plays important roles in many cellular regulations. Several synthetic peptide inhibitors and bacteria-derived inhibitors such as lactacystin and epoxomicin have been identified as potent proteasome inhibitors. However, essentially no protein proteinase inhibitor has been characterized. By examining several small size protein proteinase inhibitors, we found that a well-known serine proteinase inhibitor from bovine pancreas, basic pancreatic trypsin inhibitor (BPTI), inhibits the 20S *in vitro* and *ex vivo*. Inhibition of the 20S by BPTI was time- and concentration-dependent, and stoichiometric. To inhibit the 20S activity, BPTI needs to enter into the interior of the 20S molecule. The molar ratio of BPTI to the 20S in the complex was estimated as approximately six BPTI to one 20S, thereby two sets of three peptidase activities (trypsin-like, chymotrypsin-like and caspase-like) of the 20S were all inhibited. These results indicate that an entrance hole to the 20S formed by seven α-subunits is sufficiently large for BPTI to enter. This report is essentially the initial description of the inhibition of a threonine proteinase by a protein serine proteinase inhibitor, suggesting a common mechanism of inhibition between serine and threonine proteinases by a natural protein proteinase inhibitor.

Key words: 20S proteasome, α_1-antitrypsin, BPTI, cross-class inhibition, proteinase inhibitor.

Abbreviations: 20S, 20S proteasome; α_1-AT, α_1-antitrypsin; BBI, soybean Bowman-Birk inhibitor; BPTI, bovine pancreatic trypsin inhibitor; CPTI-II, *Cucurbita pepo* trypsin inhibitor II; DTT, dithiothreitol; ERAD, ER-associated degradation; LLE, carbobenzoxy-Leu-Leu-Glu-MCA; LLVY, succinyl-Leu-Leu-Val-Tyr-MCA; LRR, *t*-buthyloxycarbonyl-Leu-Arg-Arg-MCA; MCA, 4-methyl-coumaryl-7-amide; MCTI-I, *Momordica charantia* trypsin inhibitor I; MG132, carbobenzoxy-leucyl-leucyl-leucinal; NHK, null Hong Kong-type variant of α_1-antitrypsin; SFTI-I, sunflower trypsin inhibitor-I; SKLP, *Streptomyces* killer toxin-like protein.

INTRODUCTION

The proteasome is a key enzyme in intracellular protein turnover (*1*, *2*), antigen processing of MHC-I antigen presentation (*3*), quality control of newly synthesized proteins and degradation of malfolded glycoproteins in the endoplasmic reticulum (referred to as ERAD) (*4*), and many other cellular events (*5*, *6*). The 20S proteasome (20S), a threonine proteinase and a member of the N-terminal nucleophile–amidohydrolase family, is a major cytosolic proteinase complex forming the core of the 26S proteasome that selectively degrades ubiquitinated proteins in an ATP-dependent manner (*7*, *8*). This 750 kDa proteinase is composed of 28 subunits arranged in four heptameric stacking rings, $\alpha_7\beta_7\beta_7\alpha_7$, and forms a hollow cylindrical-shape particle. The 20S has three different peptide bond hydrolyzing activities, designated as chymotrypsin-like, trypsin-like and caspase-like activities, and attributed to β5, β2 and β1 subunits, respectively (*9*, *10*).

The 20S is a tubular molecule with the proteolytic active sites on the inner surface. Thus, substrate molecules have to be translocated through the internal cavity to the catalytic sites. However, the entrance hole for substrates, the central channel of the outer rings made of seven α-subunits, has been shown by X-ray crystallographic analysis to be too narrow to allow passage of folded proteins (*11–13*). Protein substrates need to be unfolded with reduced disulfides in order to undergo proteolytic cleavage by the 20S. In this regard, it has been reported that unfolded protein substrates (β-casein, α-synuclein, CDK inhibitor p21) are degraded by the 20S, but folded protein substrates are not degraded (*14*, *15*). However, recently we found that a 9 kDa SKLP (*Streptomyces* killer toxin-like protein) isolated from the culture supernatant of the *Streptomyces* sp, F-287 (*16*) was a good substrate for the 20S (manuscript in preparation). The results of that study led us to examine whether or not a native protein proteinase inhibitor with a molecular mass of less than 9 kDa may be able to

*To whom correspondence should be addressed. Tel: +81-791-58-0212, Fax: +81-791-58-0219, E-mail: koide@sci.u-hyogo.ac.jp

enter the inside of the 20S through a narrow gate, reach the catalytic sites and inhibit its multiple peptidase activities. Many studies on proteasome inhibitors using synthetic peptide inhibitors and/or small molecules of bacteria origin have been reported, but little is known about protein proteasome inhibitors. An additional interest was whether a protein serine proteinase inhibitor can inhibit a threonine proteinase, as cross-class inhibitions of proteinases by natural proteinase inhibitors have been reported for several serpins (*17–20*). However, there is no information as to whether a protein serine proteinase inhibitor can inhibit a threonine proteinase.

Bovine basic pancreatic trypsin inhibitor (BPTI) is a 6.5-kDa proteinase inhibitor known to inhibit many serine proteinases, including trypsin, chymotrypsin, kallikrein, etc., by forming a Michaelis-type complex with a target proteinase (*21*). Here, we demonstrate that BPTI can translocate through a putative narrow opening in the α-ring formed by seven α-subunits of the 20S, and can inhibit all three peptidase activities of the proteasome. We also demonstrate that inhibition of the 20S by BPTI is stoichiometric and competitive. Furthermore, we demonstrate that the intracellular degradation of a mutant α1-antitrypsin by the proteasome is suppressed by BPTI co-expressed in HEK293 cells. Although inhibitory effects of BPTI and soybean trypsin inhibitor (Mr 20,100) on the proteasome-like serine proteinase from lobster muscle have been previously reported, no detail of inhibition was demonstrated (*22*, *23*). Accordingly, to our knowledge, this is the first report demonstrating the stoichiometric, competitive inhibition of a threonine proteinase by a protein serine proteinase inhibitor.

MATERIALS AND METHODS

Materials—Porcine liver was obtained from a local slaughter house (Shingu-cho, Hyogo, Japan). Chromatography media were purchased all from Amersham Biosciences (Uppsala, Sweden). Various peptidyl 4-methyl-coumaryl-7-amide (MCA) substrates, succinyl-Leu-Leu-Val-Tyr-MCA (LLVY), *t*-buthyloxycarbonyl-Leu-Arg-Arg-MCA (LRR), carbobenzoxy-Leu-Leu-Glu-MCA (LLE) and carbobenzoxy-leucyl-leucyl-leucinal (MG132) were purchased from Peptide Institute (Osaka, Japan). BPTI (also known as aprotinin, Mr = 6,500) was purchased from TAKARA BIO INC (Shiga, Japan). SFTI-I (sunflower trypsin inhibitor-I, Mr = 1,500) was isolated from sunflower seeds (*24*). BBI (soybean Bowman-Birk inhibitor, Mr = 7,850), BBI F-C (chymotrypsin inhibitor fragment of BBI, Mr = 3,150), E-I (soybean BBI-type trypsin inhibitor, Mr = 7,200) and BSI (barley subtilisin inhibitor, Mr = 7,200) were kindly provided by Dr Shoji Odani (Niigata University) and MCTI-I (*Momordica charantia* (bitter gourd) trypsin inhibitor I, Mr = 3,500) by Dr Kaeko Kamei (Kyoto Institute of Technology). Flamingo™ fluorescent gel stain was purchased from Bio-Rad Labs (Hercules, CA). Reagents for cell culture were from Gibco BRL Life Technologies (Rockville, MD). Lipofectamine™ 2000 was purchased from Invitrogen (Carlsbad, CA). Zysorbin™ (Fixed and killed *Staphylococcus aureus* Protein A pos. strain) was from Zymed Labs (San Francisco, CA). [^{35}S]Methionine/cysteine (NEG-772) was from Perkin-Elmer (Boston, MA). Sodium lauryl sulfate (SDS) and dithiothreitol (DTT) were purchased from Nacalai Tesque (Kyoto, Japan). All other reagents and chemicals used in these experiments were of the highest grade commercially available and obtained from Wako Pure Chemicals Industries (Osaka, Japan) or Nacalai Tesque.

Proteasome Purification—In this study, we purified and characterized porcine and rat 20S. However, since the purification procedure and the results were essentially the same for both 20S preparations, only those experiments and results of the porcine 20S are described here in. The 20S was purified from porcine liver according to a previously published protocol with a slight modification (*25*). Porcine liver was perfused with a 0.25 M sucrose solution and then washed with 20 mM phosphate buffer, pH 7.4, containing 0.15 M NaCl (PBS). The washed liver was homogenized in nine volumes of 20 mM Tris–HCl buffer, pH 7.5, containing 50 mM KCl, 2 mM $MgCl_2$ and 0.25 M sucrose (homogenization buffer). After centrifugation for 20 min at 12,000 × *g*, the supernatant was recovered and subsequently ultracentrifuged for 1 h at 105,000 × *g*. The resulting cytosol fraction (supernatant) was fractionated with ammonium sulfate (30–70% saturation). The precipitated protein was collected by centrifugation for 20 min at 12,000 × *g*, and dissolved in 50 mM Tris-HCl buffer, pH 7.5, containing 1 mM EDTA, 1 mM benzamidine and 1 mM DTT. Hereafter, 1 mM DTT was included in all the purification steps. However, DTT was not used, unless otherwise stated, in those experiments using the purified 20S. The solution was dialysed against 50 mM Tris–HCl buffer, pH 7.5, containing 1 mM EDTA, 1 mM benzamidine, 1 mM DTT and 0.25 M sucrose (buffer A). After dialysis, the soluble sample was applied to a DEAE-Sepharose column (100 ml) equilibrated with buffer A. After washing the column with buffer A, bound materials were eluted with 500 ml each of a linear gradient of 0–0.4 M NaCl in the same buffer. Chymotryptic activity of each fraction was assayed and active fractions were pooled and applied to an SP-Sepharose column (50 ml) equilibrated with 50 mM acetate buffer pH 5.5, containing 1 mM EDTA, 1 mM DTT and 0.25 M sucrose (buffer B). Bound materials were eluted with 250 ml each of a linear gradient of 0–0.3 M NaCl in buffer B. The active fractions were pooled, applied to a Poros-HS column (1.6 ml) equilibrated with buffer B and bound materials were eluted with 30 ml each of a linear gradient of 0–0.4 M NaCl in buffer B. The active fractions, pooled and concentrated by ultrafiltration with a CENTRICON YM-30 (MILLIPORE), were applied to a Superdex 200 column (10 × 300 mm) equilibrated with buffer A containing 150 mM NaCl. Then, active fractions were applied to a Poros-HQ column (1.6 ml) equilibrated with buffer A. After washing with the same buffer, bound materials were eluted with 30 ml each of a linear gradient of 0–0.6 M NaCl in buffer A. To examine the purity of the 20S preparation, fractionated samples were subjected to SDS–PAGE. The 20S thus purified was desalted and stored at –80°C in 20% glycerol until use. Poros-HS and Poros-HQ column chromatographies were performed

using a BioCAD 700E-HT (PerSeptive). Superdex 200 gel filtration was performed using an FPLC system (Pharmacia). Fractions eluted from each column were monitored by measuring both absorbance at 280 nm and LLVY-hydrolyzing activity in the presence of 0.02% SDS.

Assay of Peptidase Activity—An aliquot of the sample (10 μl) was added to 90 μl of a fluorogenic substrate solution such that the final reaction mixture was composed of 50 μM MCA substrate in 50 mM Tris-HCl buffer-1 mM EDTA, pH 7.5 in the presence of 0.020% SDS-10% glycerol (in cases of LLVY and LLE) and in the absence of SDS (in case of LRR), and/or 1 mM DTT. After a 10 min incubation at 37°C, the reaction was stopped by the addition of 150 μl of 1 N acetic acid. The mixture was made up 1 ml with distilled water, and the fluorescence of the released 7-amino-4-methylcoumarin (AMC) was measured with excitation at 380 nm and emission at 440 nm using an F-3010 fluorescence spectrophotometer (Hitachi).

Inhibitions of the Purified 20S Proteasome by Various Protein Proteinase Inhibitors—The inhibitory activity of a proteinase inhibitor was assayed by quantifying the decrease of hydrolysis of synthetic peptidyl MCA substrate by the 20S. The 20S (60 nM) and increasing amounts of inhibitors (0–16 μM) in 50 mM Tris–HCl buffer, pH 7.5, containing 1 mM EDTA and 10% glycerol were incubated for 0–60 min at 37°C. At selected time intervals, an aliquot of sample (10 μl) was withdrawn and added to 90 μl of the fluorogenic substrate solution and the residual 20S activity was determined as described above. The reaction of the 20S and inhibitor was performed in the presence of 0.020% SDS (for the 20S activation). For experiments in the presence of 0.020% SDS, 1/10 volume of 0.22% SDS solution was added prior to incubation.

Kinetic Analysis—Determination of the type of inhibition was based on analyses of the Michaelis-Menten kinetic parameters of control and BPTI-20S reactions, using a fluorogenic peptide substrate (LLVY). The type of inhibition was determined by Lineweaver–Burk plots constructed in the presence of several different concentrations of BPTI.

Stoichiometric Analysis of Inhibition—The ratio of BPTI associated with the 20S was determined by isolating the 20S-BPTI complex by Superdex75 gel filtration, followed by SDS–PAGE analysis. First, the 20S (65 nM) and excess amounts of BPTI (6.5 μM) was incubated for 60 min at 37°C in 50 mM Tris–HCl buffer, pH 7.5, containing 1 mM EDTA, 10% glycerol and 0.025% SDS. The reaction mixture was then applied to a Superdex75 column (10 × 300 mm) equilibrated with this buffer, and the peak fraction of the 20S-BPTI complex at the void volume was subjected to SDS–PAGE analysis. SDS–PAGE was performed by the method of Schägger and von Jagow in 15% gels containing 0.1% SDS using a Tris–tricine buffer system (*26*). Gels were stained with Flamingo™ fluorescent gel stain, and fluorescence of the preparation was measured with an FLA-3000G, Image Reader V1.8J, Image Gauge V3.41 (FUJIFILM). The ratio of BPTI complexed with the 20S was calculated from the fluorescence value by interpolation from a standard curve.

Cell Culture and Transfection of HEK293 Cells—HEK-293 cells were cultured in 6-well tissue culture plates containing Dulbecco's Modified Eagle Medium (DMEM) supplemented with 10% fetal bovine serum (FBS). Cells were grown at 37°C in a humidified atmosphere containing 5% CO_2, and then transiently transfected using Lipofectamine™ 2000 in the absence of serum. Transfection efficiencies were normalized by co-expression of enhanced green fluorescent protein (EGFP). Expression vector, pEB6-NHK-IGFP was constructed by inserting a PCR fragment of α_1-AT-null Hong Kong-type variant (NHK) into pEB6MCS-IRESEGFP digested with EcoRI.

Pulse-Chase Experiments—Following transfection, NHK-expressing cells were cultured for 24 h under standard conditions. For pulse-chase experiments, cells were starved for 30 min in methionine-free medium containing 10% FBS, and then pulse-labelled for 30 min in the same medium supplemented with 100 μCi/ml [^{35}S]Met/Cys (NEG-772). At the end of pulse-labelling, cells were washed and chased for the indicated times with complete medium containing methionine. Either epoxomicin, a specific proteasome inhibitor, or BPTI was added to the culture medium during the chase period. At selected times, cells were lysed in 600 μl of 10 mM Tris–HCl buffer, pH 7.4, containing 0.1% SDS, 1% Nonidet P-40, 150 mM NaCl, 1 mM EDTA, 0.1 mM PMSF and 1 μg/ml each of leupeptin and BPTI. NHK was immunoprecipitated with goat anti-human α1AT IgG, and the precipitates were recovered by the addition of Zysorbin. After washing, immunoadsorbed NHK was dissociated from IgG by heating, and subjected to SDS–PAGE. The gels were dried and the radioactivity of NHK was measured with an FLA-3000G, Image Reader V1.8J, Image Gauge V3.41 (FUJIFILM).

Co-Expression of BPTI and α_1-AT NHK (NHK)—For co-expression of BPTI and NHK, an expression vector, pEB6-BPTI-IGFP, was constructed using PCR amplicon of the BPTI cDNA without a nucleotide sequence coding for a signal sequence, and co-transfected into HEK293 cells together with an NHK expression vector.

RESULTS

Effects of Protein Proteinase Inhibitors on the Peptidase Activity of the 20S Proteasome In Vitro—We have previously discovered SKLP as a good substrate for the 20S. Interestingly, native SKLP was degraded by the SDS-activated 20S, which suggested to us that protein proteinase inhibitors with a molecular weight of 9,000 may be able to get through the narrow entrance, reach the inner catalytic sites, and inhibit the peptidase activities of the 20S. Low concentrations of SDS (0.020%) stimulate peptide cleavages by the latent 20S, except for cleavage of *boc*-LRR-MCA by the trypsin-like catalytic sites (*27*). Because SDS is known to activate the 20S by inducing a conformational change in the enzyme that allows substrates easier access to the catalytic sites, SDS is commonly used to assay the 20S activities *in vitro*. However, it is also known that this 'activation' by SDS results in an enhanced inactivation of the proteasome activity because of the lability of the activated

conformation. Consequently, we established optimal conditions for long-term stable incubation of purified 20S with substrates/inhibitors. (described in MATERIALS AND METHODS).

We initially screened several low-molecular weight protein proteinase inhibitors for their potential inhibitory effects on the trypsin-like peptidase activity of the 20S. A 20S solution (60 nM), and various concentrations of inhibitors (0–16 μM), were incubated in the presence of 0.020% SDS for 60 min at 37°C. Following incubation, an aliquot was added to the fluorogenic substrate solution and the residual activity of the 20S was determined as described in MATERIALS AND METHODS. From these studies, we found that BPTI, consisting of 58 amino acid residues containing three disulfide bonds, and *Momordica charantina* trypsin inhibitor (MCTI-I), consisting of 30 amino acid residues containing three disulfide bonds, exhibited inhibitory activities against the trypsin-like peptidase activity of the 20S (Fig. 1).

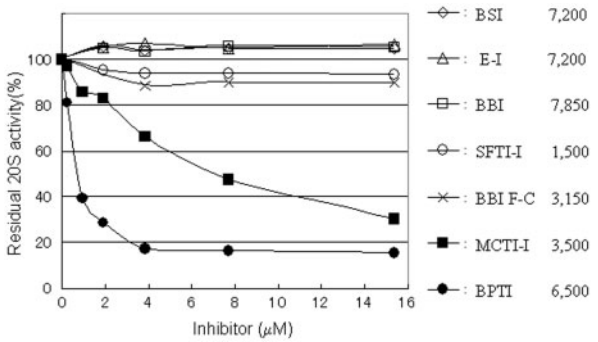

Fig. 1. **Effects of various protein proteinase inhibitors on the trypsin-like activity of the 20S.** The 20S and inhibitor (BBI, BSI, E-I, SFTI-I, BBI F-C, MCTI-I or BPTI) were incubated in the presence of 0.020% SDS for 60 min at 37°C. After incubation, the LRR-hydrolyzing activity of the 20S was measured in the absence of 0.020% SDS. 100% activity represents the activity in the absence of inhibitors, and other activities are shown as a percentage of that value.

However, CPTI-II, a trypsin inhibitor from *Cucurbita pepo* (*28*) highly homologous to MCTI-I, had no inhibitory activity against the 20S (data not shown).

Inhibition of the 20S by BPTI Is Time- and Concentration-Dependent—To further determine the inhibitory effect of BPTI on other peptidase activities of the 20S, excessive amounts of BPTI was incubated with the 20S in the presence of 0.020% SDS for 0–60 min at 37°C, and the residual 20S activity was measured using a synthetic peptidyl MCA substrate for assay of the chymotrypsin-like activity. The results showed that the 20S was inhibited by BPTI in a time- and concentration-dependent manner (Fig. 2). As a consequence, 95% of the 20S activity was inhibited by BPTI in 15 min (Fig. 2A). Moreover, a linear relationship between the extent of the 20S inhibition and the concentration of BPTI was observed until 80% inhibition, suggesting that 15 molar excess of BPTI is required to inhibit the 20S (Fig. 2B).

BPTI Invades the Interior of the 20S to Inhibit Its Peptidase Activities—It is conceivable that the apparent inhibition of the proteasome activity is because of blockage of the substrate entrance hole by BPTI. To address this possibility, we examined whether BPTI can penetrate the narrow opening of the 20S, which has been shown to be 13 Å in diameter by X-ray chrystallographic analysis (*11–13*). BPTI has three disulfide bonds: Cys14/Cys38, Cys30/Cys51, Cys5/Cys55, among which Cys14/Cys38 has been shown to be selectively reduced with as high as 10 mM DTT, and the partially reduced inhibitor retained full inhibitory activities towards both trypsin and chymotrypsin (*29–32*). Thus, we prepared the Cys14/Cys38-reduced BPTI and examined its inhibitory property against the 20S. A partial reduction was confirmed by its elution profile from a C_{18} reversed-phase HPLC column that was strikingly different from that of intact BPTI. Approximately 50 μg of BPTI was applied to a CAPCELL PAK C18 column equilibrated with 0.1% trifluoroacetic acid and eluted with a linear gradient of acetonitrile in the same solution. HPLC of the partially reduced BPTI was performed in the presence of 1 mM

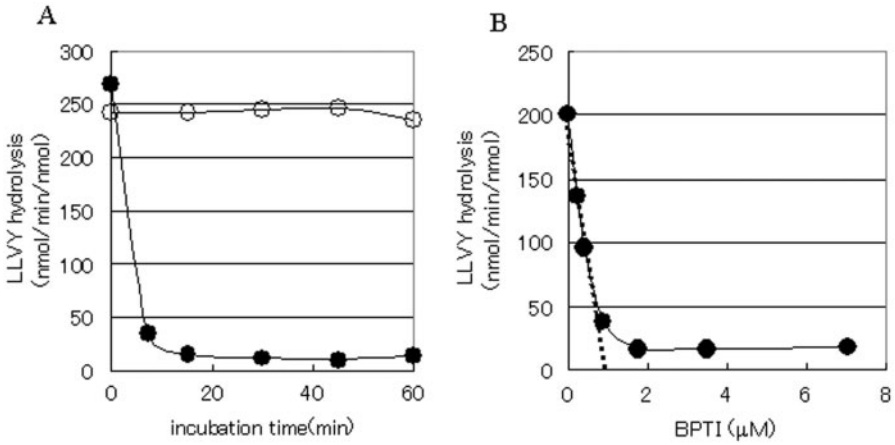

Fig. 2. **Inhibition of the 20S by BPTI is time- and concentration-dependent.** The 20S inhibition by BPTI was assessed using LLVY as a substrate. (A) The 20S (66 nM) and an excessive amount of BPTI (6.5 μM) were incubated in the presence of 0.020% SDS for 0–60 min at 37°C, and the residual 20S activity was measured as described in 'MATERIALS AND METHODS section'. Open circle, 20S only; filled circle, 20S and BPTI. (B) 20S (66 nM) and increasing amounts of BPTI were incubated for 60 min at 37°C. After incubation, each sample was assayed for the residual proteasome activity in the presence of 0.020% SDS.

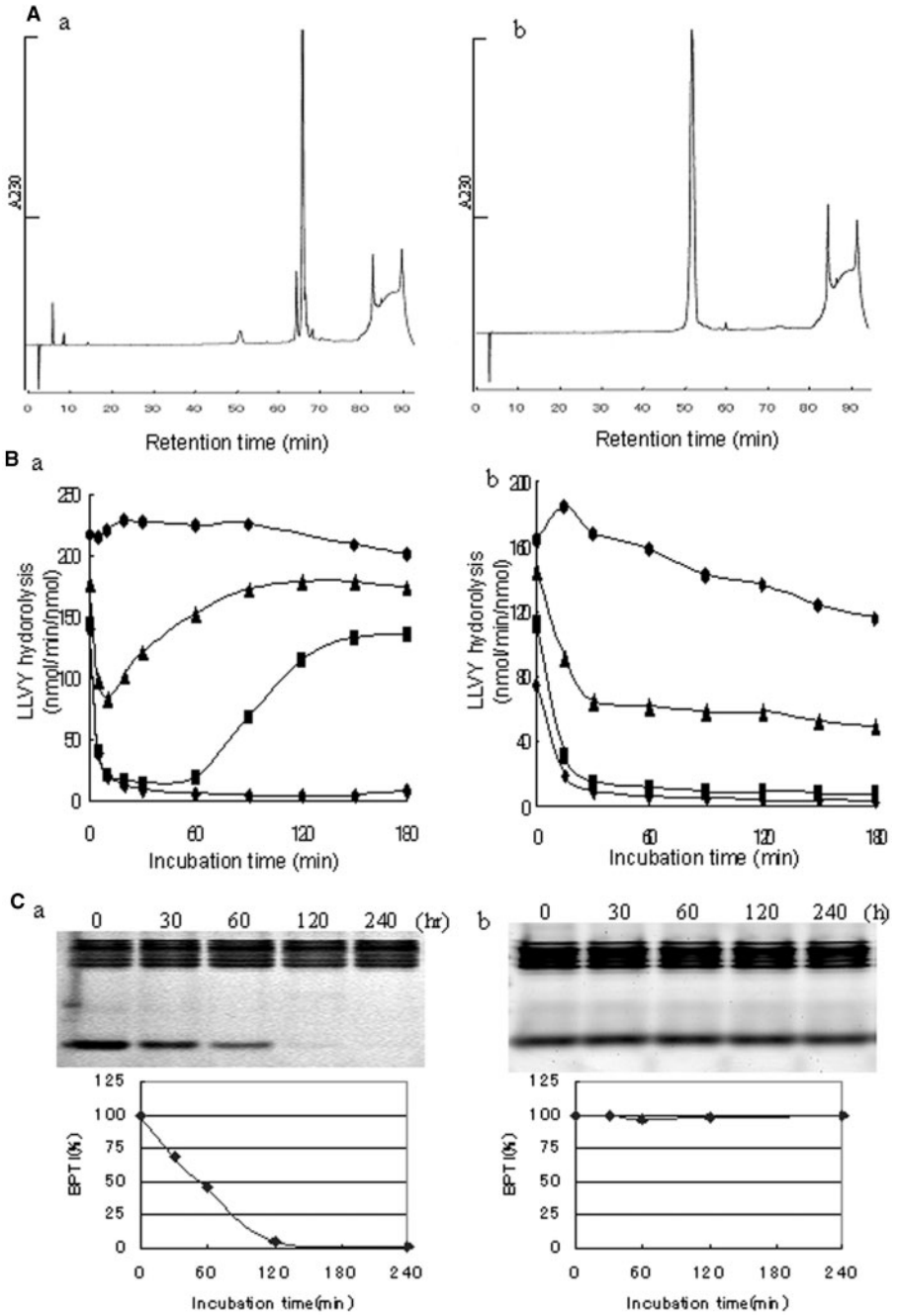

Fig. 3. **BPTI invades the inside of the 20S to inhibit its activities.** (A) Reversed-phase HPLC of the partially-reduced BPTI in the presence of 1 mM DTT (a) and that of the intact BPTI without DTT (b). Peaks were monitored by measuring absorbance at 230 nm. (B) Inhibition of the 20S by the partially-reduced BPTI assayed in the presence of 1 mM DTT (a) and by the intact BPTI (b). circle, control 20S; triangle, BPTI:20S = 25:1 (mole/mole); square, 50:1; diamond, 100:1. (C) Partially reduced BPTI (a) or intact BPTI (b) and the 20S were incubated for 240 min at a molar ratio of 50:1, and an aliquot was withdrawn at indicated time intervals and subjected to SDS–PAGE analysis. Taking the intensity of BPTI band at 0 time incubation as 100%, the relative intensity of BPTI band at each incubation time was shown on lower graphs.

DTT in all solutions. The Cys14/Cys38–reduced BPTI eluted with a retention time of 66 min (at a concentration of 35% acetonitrile) (Fig. 3A-a), while the intact BPTI eluted with a retention time of 51 min (at a concentration of 25% acetonitrile) (Fig. 3A-b). The inhibitory activities of BPTI and its reduced derivative were compared by the quantitative inhibition of LLVY hydrolysis by the 20S. To preserve its reduced form, the assay of the reduced BPTI was performed in the presence of 1 mM DTT. The 20S was incubated with 25, 50 and 100 molar excess of either BPTI or its derivative for 0–180 min at 37°C. The partially reduced BPTI appeared to inhibit the 20S at the same rate and intensity as the intact BPTI in the early stage of

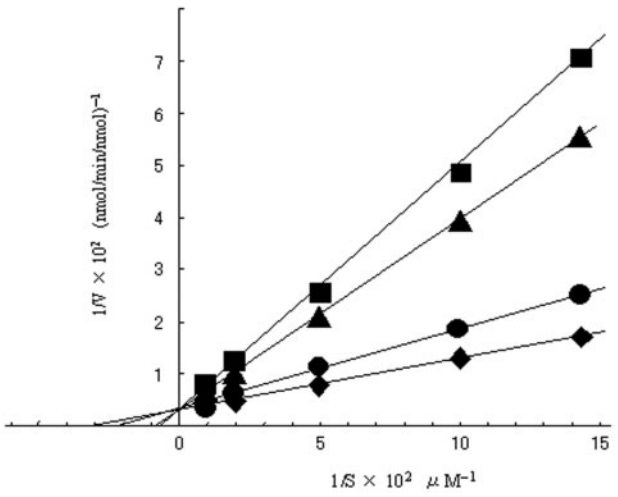

Fig. 4. **BPTI competitively inhibits the chymotrypsin-like activity of the 20S as shown by Lineweaver–Burk plot.** The LLVY-hydrolyzing activity of the 20S in the presence of different concentrations of BPTI was analysed by the initial velocity assay in Tris–HCl, pH 7.5, containing 0.020% SDS at 37°C. Circle, 20S with no BPTI (control); triangle, square and diamond indicate a molar ratio of BPTI to 20S = 25, 50 and 100 to 1, respectively.

incubation, but on prolonged incubation, the peptidase activity of the 20S reappeared, revealing a temporary inhibition-like spectrum (Fig. 3B-a), in contrast to the permanent inhibition by the intact BPTI (Fig. 3B-b). This phenomenon was further assessed by SDS–PAGE, which revealed that the partially reduced BPTI has been degraded time-dependently by the 20S (Fig. 3C-a), whereas the intact BPTI was not degraded (Fig. 3C-b). These results strongly suggest that BPTI invades the interior of the 20S and inhibits its peptidase activities.

Inhibition of the 20S by BPTI Is Competitive—Since BPTI is known as a serine proteinase inhibitor that interacts with the serine residue at the active site of a serine proteinase, it was of interest to examine whether BPTI directly interacts with the active sites of the 20S. As a first step, we examined the mode of inhibition of the 20S by BPTI. Determination of the type of inhibition was based on analysis of the Michaelis–Menten kinetic parameters in the reaction between BPTI and the 20S using a fluorogenic peptide (LLVY) as a substrate. Analyses of Lineweaver–Burk plots revealed that the inhibition was competitive with a K_i value of 2×10^{-6} M (Fig. 4).

Effects of SDS on the Inhibition of the 20S by BPTI and Other Inhibitors—The 20S is a tubular complex with the active sites on the inner surfaces such that large substances should be sterically hindered from reaching the active sites. Thus, we predict that opening of the 20S channel may enhance the inhibition of the 20S by proteinase inhibitors. To test this, we examined the inhibition of the 20S by BPTI in the presence and absence of SDS. The 20S was preincubated with 0.02% SDS for 10 min at 37°C prior to incubation with epoxomicin, MG132 or BPTI for 1 h, and the remaining activity subsequently assayed as described in 'MATERIALS AND METHODS'.

These three inhibitors potently inhibited the chymotrypsin-like activity of the SDS-activated 20S (Fig. 5A). In contrast, the inhibition of the latent 20S (in the absence of SDS) by these inhibitors was several-fold weaker than that of the activated form. Thus, SDS treatment significantly enhanced the sensitivity of this particular catalytic site to these inhibitors. It is noteworthy that SDS had similar effects on the 20S inhibition both by typical low molecular weight proteasome inhibitors and by BPTI. Furthermore, BPTI was a more potent inhibitor than MG132 of synthetic substrate-hydrolyzing activities when α-ring channel(s) were in their open states. This greater inhibitory potency of BPTI in the open gate form of the 20S may simply reflect the fact that the conformational change of the α-ring-forming subunits allows easier access of substances to the catalytic sites, although additional allosteric effects cannot be ruled out. BPTI inhibited the caspase-like activity with maximal inhibition of 86% at a concentration of 2 μM (Fig. 5B-a), and the trypsin-like activity with maximal inhibition of 82% at a concentration of 4 μM (Fig. 5B-b). IC_{50} values for these inhibitors in the inhibition of three different 20S activities are listed in Table 1. It is interesting to note that BPTI inhibits the caspase-like activity more potently than the typical proteasome inhibitors, epoxomicin and MG132.

Stoichiometric Analysis of Complex Formation—Kinetic experiments indicated that BPTI interacts with the catalytic sites of the 20S that exist on the inner side of the tubular molecule. To directly demonstrate the interaction between BPTI and the catalytic sites of the 20S, we isolated the 20S–BPTI complex by gel filtration using Superdex 75. A large peak was eluted at a position corresponding to a size of ~700 kDa (void volume) where the 20S was eluted (Fig. 6A). About 90% of the original 20S activity was inhibited by BPTI before gel filtration and more than 90% of the 20S activity had been lost in the large peak fraction that contained the complex of the 20S and BPTI (Fig. 6B and far left lane in 6C). A portion of the large peak fraction containing the 20S-BPTI complex was subjected to SDS–PAGE analysis together with known amounts of the 20S and BPTI for semi-quantitative determination of the molar ratio of BPTI to the 20S in the complex (far left lane of SDS–PAGE in Fig. 6C). This ratio was calculated as 5.1 to 1 from the fluorescence value using a standard curve, suggesting that about six molecules of BPTI have been incorporated into one 20S molecule.

Effect of BPTI on the ERAD of a Null Hong Kong-Type Variant of α_1-Antitrypsin—We next confirmed the inhibition of the proteasome activity by BPTI by *ex vivo* experiments. For this purpose, we examined the inhibitory effect of BPTI on intracellular degradation of a misfolded glycoprotein by pulse-chase experiments using HEK293 and BHK cells. Misfolded glycoproteins are retro-translocated from the ER to the cytosol through the dislocon and degraded by the ubiquitin-proteasome system known as ER-associated degradation (ERAD) (*33*, *34*). As a substrate for ERAD, we used a null Hong Kong-type variant of α_1-antitrypsin (α_1-AT NHK), as it has been well established that α_1-AT NHK expressed in HEK293 or BHK cells is degraded by the proteasome

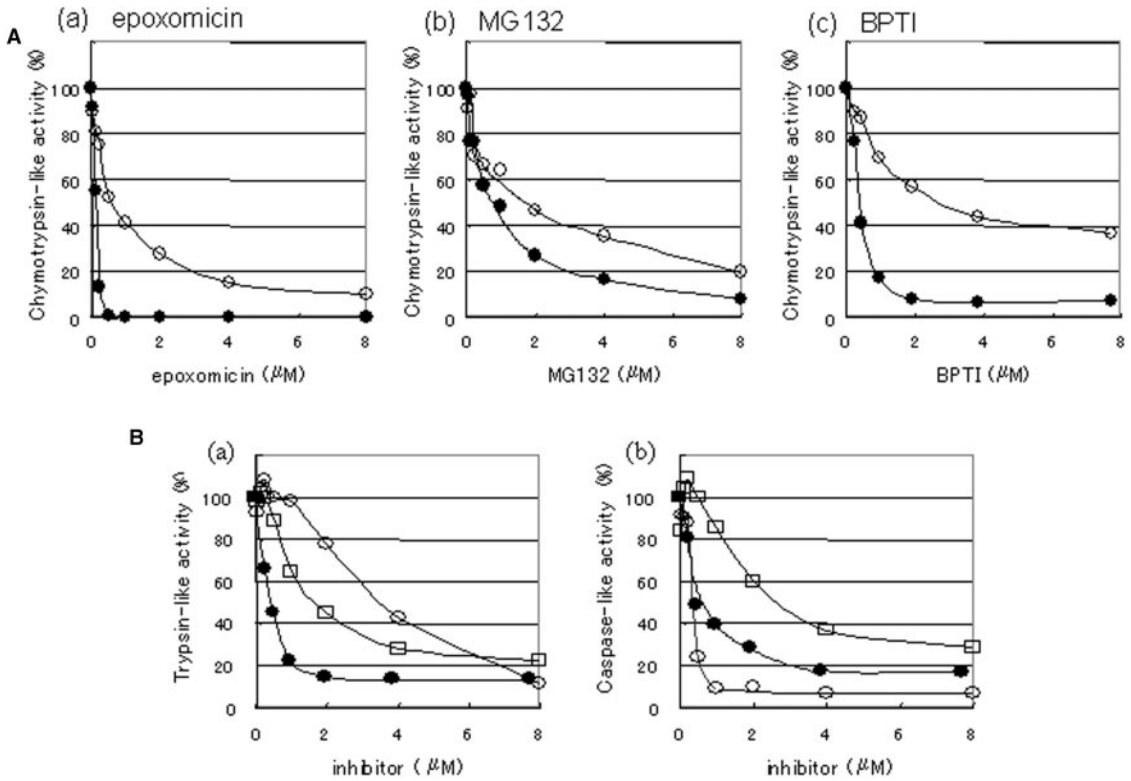

Fig. 5. **Comparison of three inhibitors in the inhibitions of three peptidase activities of the 20S.** (A): SDS-dependent enhancement of the 20S inhibition by typical proteasome inhibitors and BPTI; (a) epoxomicin, (b) MG132, (c) BPTI. Filled circle, hydrolysis of LLVY in the presence of 0.020% SDS; open circle, hydrolysis of LLVY in the absence of SDS. (B) Effects of inhibitors on the caspase-like activity of the 20S to hydrolyse LLE (a) and the trypsin-like activity to hydrolyse LRR (b). The 20S (66 nM) was incubated with different concentrations of each inhibitor in the presence of 0.020% SDS for the caspase-like activity assay and in the absence of SDS for the trypsin-like activity assay. The 20S activity in the absence of inhibitors was taken as 100%, and other activities are expressed by the relative values. (Filled circle) BPTI, (open circle) epoxomicin and (open square) MG132.

Table. 1. **Calculated IC_{50} values for MG132, epoxomicin and BPTI.**

Inhibitor	IC_{50} (μM)		
	β5 Chymotrypsin-like	β2 Trypsin-like	β1 Caspase-like
MG132	0.78	2.3	1.7
epoxomicin	0.14	0.32	3.6
BPTI	0.42	0.79	0.53

IC_{50} values were calculated from inhibition of the 20S (66 nM) with increasing amounts of inhibitors in the presence of 0.02% SDS.

(ubiquitin-proteasome system), and small proteasome inhibitors (MG132, epoxomicin and lactacystin) suppressed the ERAD of α_1-AT NHK (*35*). HEK293 cells expressing α_1-AT NHK were pulse-labelled with 100 μCi/ml [^{35}S]methionine/cysteine for 30 min and subsequently chased for 4 h in the absence and presence of either BPTI or epoxomicin. α_1-AT NHK in the cell extracts were immunoprecipitated, electrophoresed and quantified by its radioactivity. The results showed that, in the presence of BPTI, the degradation of α_1-AT NHK after a 4 h-chase was obviously suppressed in a BPTI concentration-dependent manner when BPTI was added to the culture medium during the chase period (Fig. 7). Finally, to confirm the inhibitory effect of BPTI on the intracellular proteasome, we co-expressed signal sequence-removed BPTI (see 'MATERIALS AND METHODS' section) and α_1-AT NHK in HEK293 and BHK cells. In both cases, ERAD of α_1-AT NHK was significantly suppressed in a time-dependent manner in the cells expressing BPTI (Fig. 8) (Results of BHK cells are not shown).

DISCUSSION

In this study, we examined several protein proteinase inhibitors for their inhibitory effects on the peptidase activities of the 20S proteasome. The molecular mass range of these proteinase inhibitors was between 1,500 and 8,000 Da. These inhibitors present their reactive site on an exposed loop and react with the target enzyme according to a pseudo-substrate mechanism. Among them, we found that BPTI and MCTI-I had definite inhibitory activities against the trypsin-like activity of the 20S (Fig. 1). At first, we anticipated that inhibitors with a smaller molecular weight would interact more easily with the 20S. However, sunflower trypsin inhibitor (SFTI-I), the smallest inhibitor consisting of a 14-amino-acid residue cyclic peptide and a potent inhibitor of trypsin (K_i = 100 pM) (*24*), failed to exhibit any

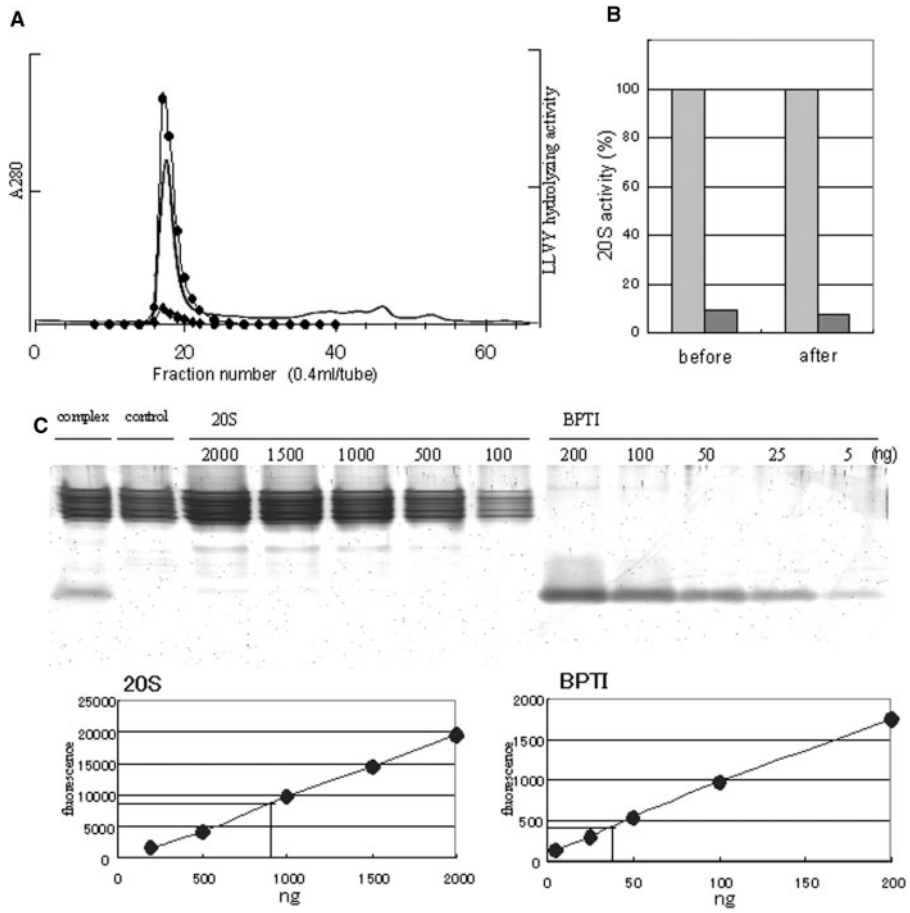

Fig. 6. **Stoichiometric analysis of complex formation.** (A) Isolation of the 20S-BPTI complex by gel filtration on Superdex 75 was performed using an FPLC system. An aliquot (10 μl) of each fraction from the column was assayed for 20S activity using LLVY as a substrate. Solid circle and diamond indicate the activities of the fractions of the 20S and the 20S-BPTI complex, respectively. (B) The relative 20S activities before and after gel filtration. Light grey, 20S without BPTI; dark grey, 20S incubated with BPTI. (C) Semi-quantitative analysis of the 20S-BPTI complex formation by SDS–PAGE. SDS–PAGE was performed by the method of Schägger and von Jagow in 15% gels containing 0.1% SDS using a Tris-tricine buffer system (*26*). The gels were stained with Flamingo™ fluorescent gel stain. Samples from left to right lanes: 20S-BPTI complex, 20S without BPTI (control), standard 20S (each containing 2,000, 1,500, 1,000, 500 and 100 ng), and standard BPTI (each containing 200, 100, 50, 25 and 5 ng).

inhibitory activity against the 20S. It is interesting to note that the 20S from *Methanosarcina thermophila* cleaved tripeptide substrates linked with variable chain length of PEG (Mr 1,000–5,000) more efficiently than free *suc*-Ala-Ala-Phe-*p*-nitroanilide (*36*). At present, however, it is unclear to us whether SFTI-I could not penetrate the inside of the 20S, or whether it simply could not inhibit the trypsin-like activity of the 20S after reaching its catalytic sites. Interestingly, MCTI-I inhibited the trypsin-like activity of the 20S, whereas *Cucurbita pepo* trypsin inhibitor (CPTI-II) (*37*), a homolog from summer squash, did not exhibit any inhibitory activity. The amino acid sequences of these two Bowman-Birk-type inhibitors are well conserved, being that 24 of 29 residues are the same or conservative residues. The reactive site of MCTI-I is located within an eight-residue loop with a disulfide bond between Cys4 and Cys11. Six of eight residues are the same or conservative between the two inhibitors. However, there is a notable difference of two amino acid residues within the reactive site loop (P1′–P4′) [The terminology of the reactive site residue positions is taken from Schechter and Berger (1967) *Biochem. Biophys. Res. Commun.* **27**, 157–162.] sequence is Ile-Leu-Lys-Gln in MCTI-I and Ile-Leu-Met-Glu in CPTI-II) that may confer the inhibitory specificity. The difference between Lys-Gln and Met-Glu might be crucial for the inhibitory and non-inhibitory properties, respectively, of these homologous inhibitors against the 20S. Furthermore, the presence of a basic residue in the P2′ or P3′ position seems to be important in the interaction with S3 pocket of the β2 subunit of the 20S. In contrast to Arg-Ile and Leu-Lys for the P2′ and P3′ residues in BPTI and MCTI-I, respectively, the corresponding sequences are Ile-Pro and Leu-Met in SFTI-I and CPTI-II, respectively, even though the P1 residue is Lys in both BPTI and SFTI.

Hitherto, PI31 (*38*) and PR-rich peptides (*39*) have been reported as protein proteasome inhibitors. However, the mode of inhibition by these inhibitors is not through the interaction with the catalytic sites of the proteasome,

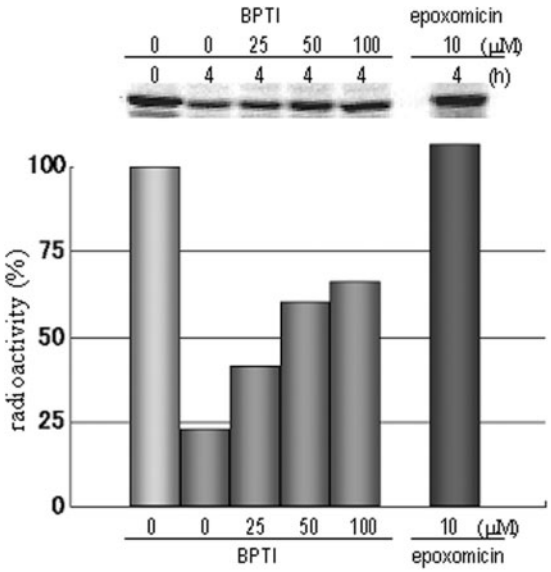

Fig. 7. **Effect of BPTI on the ERAD of the null Hong Kong-type variant of α1-antitrypsin (α1-AT NHK).** (A) HEK293 cells expressing α1-AT NHK were pulse-labelled with 100 μCi/ml [^{35}S]methionine/cysteine for 30 min and subsequently chased for 4 h in the presence of various concentrations (0–100 μM) of BPTI or epoxomicin (10 μM). α1-AT NHK in the cell extracts were immunoprecipitated, electrophoresed and quantified by radioactivity measurements following gel drying. Taking the radioactivity of the pulse-labelled α1-AT NHK at the 0 h chase period as 100%, the relative radioactivities after 4-h chase are shown.

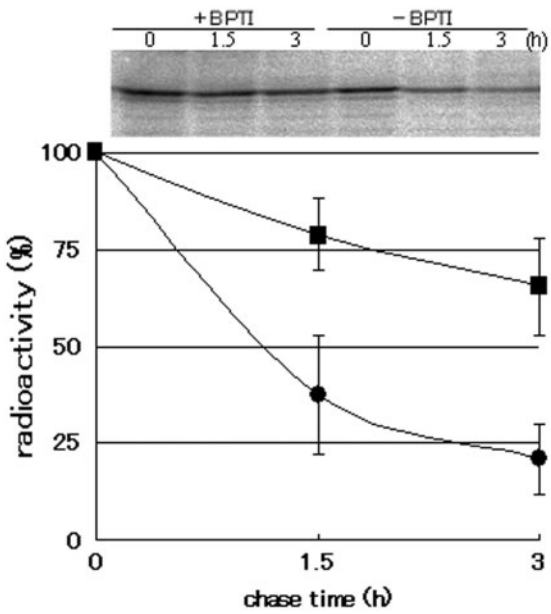

Fig. 8. **Effect of co-expression of BPTI on the ERAD of α1-AT NHK in HEK293.** BPTI- and α1-AT NHK-cotransfected HEK293 cells were pulse-labelled with 100 μCi/ml [^{35}S]methionine/cysteine for 30 min and subsequently chased for 3 h. α1-AT NHK in the cell extracts were immunoprecipitated, electrophoresed and quantified by radioactivity measurements following gel drying. The relative radioactivities of α1-AT NHK at different times of chase were plotted against chase time. (Filled circle) control (α1-AT NHK without co-expression of BPTI); (filled square) α1-AT NHK co-expressed with BPTI. Values are an average of three experiments.

but rather through their abilities to block peptide substrates from penetrating the interior by covering the entrance gate like a lid. In contrast, the inhibition of the 20S by BPTI is competitive and stoichiometric with a K_i of 2×10^{-6} M. This value does not seem to agree with the result obtained in Fig. 2B that 1 μM of BPTI is sufficient to inhibit more than 85% of the peptidase activity. This difference is due to different assay methods. Because of a unique structure of the 20S, when BPTI and peptide substrate are incubated to estimate a competitive inhibition, the apparent *Ki* value becomes high as it is advantageous to a small peptide substrate and disadvantageous to BPTI to reach the catalytic sites of the 20S that are located deep inside of the cylindrical structure. The peptidase activity of the 20S was almost completely inhibited after a 15 min-incubation with 50 molar excess of BPTI (Fig. 3B). BPTI is known to be sensitive to DTT and the Cys14-Cys38 bond is selectively reduced by 1 mM DTT, retaining its full inhibitory activity (*30*, *31*, *40*). In our experiment, partially reduced BPTI in the presence of 1 mM DTT also readily inhibited the 20S, but temporarily, as it was degraded by the 20S after prolonged incubation. Degradation of the partially reduced BPTI (50 molar excess to the 20S) by the 20S took 150 min, which was much slower than the degradation rate observed for the completely reduced BPTI (data not shown), suggesting that the partially reduced BPTI preserved its intact conformation as suggested by many previous studies (*28–30*). These results, together with the observed 'temporary inhibition', would provide us with positive evidence that the active BPTI can pass through the narrow [13 Å diameter (*41*)] entrance of the α-ring and reach the catalytic sites of the β-ring of the tubular 20S. This is not because BPTI, whose size has been shown to be 19×29 Å by X-ray crystallographic analysis (*42*), is smaller than 13 Å in diameter, but the entrance gate of the 20S is flexible as shown by atomic force microscopy (*43*) and may open wider in the presence of 0.02% SDS. It is possible to argue that, in the presence of 0.02% SDS, the conformation of BPTI must be affected and BPTI denatured, which allowed BPTI to enter through the narrow entrance gate into the inside of the 20S. To exclude this possibility, we examined and confirmed that the inhibitory activity of BPTI against trypsin was well maintained under the same condition (data not shown).

We subsequently confirmed the potency of BPTI in the 20S inhibition by *ex vivo* experiments. A mimic of a genetic variant of α1-AT, α1-AT NHK, is one of the typical substrates used for ERAD studies, and known to be degraded by the proteasome (*35*, *44*). First, we demonstrated that BPTI added to the culture medium can concentration-dependently inhibit the intracellular proteasomal degradation (ERAD) of α1-AT NHK expressed in HEK293 cells (Fig. 7). Then, to exclude permeability and cell damage problems, we co-expressed the signal sequence-removed BPTI together with α1-AT NHK, and clearly demonstrated that BPTI co-expressed in HEK293 cells also significantly suppressed the ERAD of α1-AT NHK (Fig. 8).

We also compared the inhibitory spectrum of BPTI with those of two well-known low-molecular weight proteasome inhibitors, epoxomicin and MG132, in the

presence of 0.020% SDS (without SDS in case of trypsin-like activity assay using LRR). The inhibition spectra of epoxomicin and MG132 were in good agreement with those reported previously (*45*, *46*). It is noteworthy that the efficacy of inhibition of the chymotrypsin-like and trypsin-activities of the 20S by BPTI was comparable with these low molecular weight inhibitors, but its inhibitory properties of the caspase-like activity was more potent than those of epoxomicin and MG132 (Fig. 5).

The molar ratio of BPTI to the 20S in complex was calculated as 1:5.1. Therefore, the stoichiometry of inhibition would be either 1:4 or 1:6. Recent study showed that the 20S has enough space in the interior of the molecule to keep substrates prior to their degradation, e.g. folding a maximum of three green fluorescent protein molecules or four cytochrome c molecules within the cavity (*47*, *48*). Judging from these observations, it might be possible to conclude that 6 molecules of BPTI are incorporated into the 20S and inhibit all three different peptidase activities. However, there is another possible stoichiometry that 4 molecules of BPTI interact with two each of trypsin-like and chymotrypsin-like catalytic sites and the caspase-like catalytic sites on β1-subunits are hindered by steric hindrance of BPTI through the interaction with neighboring trypsin-like catalytic sites on β2-subunits. To confirm this speculation, X-ray crystallographic analysis of the BPTI–20S complex is necessary, but our efforts to crystallize the complex in the presence of 0.02% SDS have, as yet, not been successful.

Currently, two specific proteasome inhibitors from bacteria, lactacystin and epoxomicin, are widely used as they inhibit all the proteasomal activities by binding to the N-terminal Thr on the catalytic sites. In this study, we introduced two protein proteinase inhibitors as new proteasome inhibitors, although they are not physiologically relevant proteasome inhibitors. Our finding of BPTI as a 20S proteasome inhibitor not only demonstrated that the putative hole of the α-ring formed by seven α-subunits of the 20S is sufficiently large for intact proteins of small size to enter, but may also stimulate studies to search for physiologically relevant proteasome inhibitor(s) to control the 20S within cells. The results of our *ex vivo* experiments revealed that BPTI co-expressed with α1-AT NHK in HEK293 cells suppressed ERAD of α1-AT NHK by inhibiting the proteasomal activities in cells without 0.02% SDS activation. Our result strongly suggests that not all of α1-AT NHK was degraded by the 26S proteasome after ubiquitination, but also by the active 20S in cells, since it is most unlikely that active BPTI can penetrate the inside of the 26S through the entrance of the 19S regulatory particle without ubiquitination. Furthermore, our result will cast new light on the study of ERAD, since it is still controversial whether a misfolded glycoprotein, the substrate for ERAD, is degraded through a ubiquitin-dependent or independent proteasome system.

ACKNOWLEDGEMENTS

The authors are indebted to Drs Shoji Odani (Faculty of Science, Niigata University) and Kaeko Kamei (Faculty of Engineering and Design, Kyoto Institute of Technology) for kindly supplying valuable materials. The authors are also grateful to Dr Sadao Wakabayashi of our department for his helpful discussions during the course of this study.

CONFLICT OF INTEREST

None declared.

REFERENCES

1. Baumeister, W., Walz, J., Zuhl, F., and Seemuller, E. (1998) The proteasome: paradigm of a self-compartmentalizing protease. *Cell* **92**, 367–380
2. Coux, O., Tanaka, K., and Goldberg, A.L. (1996) Structure and functions of the 20S and 26S proteasomes. *Annu. Rev. Biochem.* **65**, 801–847
3. Groettrup, M., Ruppert, T., Kuehn, L., Seeger, M., Standera, S., Koszinowski, U., and Kloetzel, P.M. (1995) The interferon-gamma-inducible 11 S regulator (PA28) and the LMP2/LMP7 subunits govern the peptide production by the 20 S proteasome in vitro. *J. Biol. Chem.* **270**, 23808–23815
4. Werner, E.D., Brodsky, J.L., and McCracken, A.A. (1996) Proteasome-dependent endoplasmic reticulum-associated protein degradation: an unconventional route to a familiar fate. *Proc. Natl. Acad. Sci. USA* **93**, 13797–13801
5. Rechsteiner, M. and Hill, C.P. (2005) Mobilizing the proteolytic machine: cell biological roles of proteasome activators and inhibitors. *Trends Cell Biol.* **15**, 27–33
6. Wolf, D.H. and Hilt, W. (2004) The proteasome: a proteolytic nanomachine of cell regulation and waste disposal. *Biochim. Biophys. Acta.* **1695**, 19–31
7. Orlowski, M. and Wilk, S. (2003) Ubiquitin-independent proteolytic functions of the proteasome. *Arch. Biochem. Biophys.* **415**, 1–5
8. Matthews, W., Driscoll, J., Tanaka, K., Ichihara, A., and Goldberg, A.L. (1989) Involvement of the proteasome in various degradative processes in mammalian cells. *Proc. Natl Acad. Sci. USA* **86**, 2597–2601
9. Heinemeyer, W., Fischer, M., Krimmer, T., Stachon, U., and Wolf, D.H. (1997) The active sites of the eukaryotic 20 S proteasome and their involvement in subunit precursor processing. *J. Biol. Chem.* **272**, 25200–25209
10. Arendt, C.S. and Hochstrasser, M. (1997) Identification of the yeast 20S proteasome catalytic centers and subunit interactions required for active-site formation. *Proc. Natl Acad. Sci. USA* **94**, 7156–7161
11. Bajorek, M. and Glickman, M.H. (2004) Keepers at the final gates: regulatory complexes and gating of the proteasome channel. *Cell Mol. Life Sci.* **61**, 1579–1588
12. Forster, A. and Hill, C.P. (2003) Proteasome degradation: enter the substrate. *Trends Cell Biol.* **13**, 550–553
13. Groll, M., Bajorek, M., Kohler, A., Moroder, L., Rubin, D.M., Huber, R., Glickman, M.H., and Finley, D. (2000) A gated channel into the proteasome core particle. *Nat. Struct. Biol.* **7**, 1062–1067
14. Jin, Y., Lee, H., Zeng, S.X., Dai, M.S., and Lu, H. (2003) MDM2 promotes p21waf1/cip1 proteasomal turnover independently of ubiquitylation. *EMBO J.* **22**, 6365–6377
15. Bennett, M.C., Bishop, J.F., Leng, Y., Chock, P.B., Chase, T.N., and Mouradian, M.M. (1999) Degradation of alpha-synuclein by proteasome. *J. Biol. Chem.* **274**, 33855–33858
16. Ohki, S.Y., Kariya, E., Hiraga, K., Wakamiya, A., Isobe, T., Oda, K., and Kainosho, M. (2001) NMR structure of Streptomyces killer toxin-like protein, SKLP: further evidence for the wide distribution of single-domain betagamma-crystallin superfamily proteins. *J. Mol. Biol.* **305**, 109–120

17. Holland, L.J., Suksang, C., Wall, A.A., Roberts, L.R., Moser, D.R., and Bhattacharya, A. (1992) A major estrogen-regulated protein secreted from the liver of *Xenopus laevis* is a member of the serpin superfamily. Nucleotide sequence of cDNA and hormonal induction of mRNA. *J. Biol. Chem.* **267**, 7053–7059
18. Takeda, A., Yamamoto, T., Nakamura, Y., Takahashi, T., and Hibino, T. (1995) Squamous cell carcinoma antigen is a potent inhibitor of cysteine proteinase cathepsin L. *FEBS Lett.* **359**, 78–80
19. Annand, R.R., Dahlen, J.R., Sprecher, C.A., De Dreu, P., Foster, D.C., Mankovich, J.A., Talanian, R.V., Kisiel, W., and Giegel, D.A. (1999) Caspase-1 (interleukin-1beta-converting enzyme) is inhibited by the human serpin analogue proteinase inhibitor 9. *Biochem. J.* **342 (Pt 3)**, 655–665
20. Komiyama, T., Ray, C.A., Pickup, D.J., Howard, A.D., Thornberry, N.A., Peterson, E.P., and Salvesen, G. (1994) Inhibition of interleukin-1 beta converting enzyme by the cowpox virus serpin CrmA. An example of cross-class inhibition. *J. Biol. Chem.* **269**, 19331–19337
21. Fioretti, E., Iacopino, G., Angeletti, M., Barra, D., Bossa, F., and Ascoli, F. (1985) Primary structure and antiproteolytic activity of a Kunitz-type inhibitor from bovine spleen. *J. Biol. Chem.* **260**, 11451–11455
22. Mykles, D.L. (1989) High-molecular-weight serine proteinase from lobster muscle that degrades myofibrillar proteins. *J. Exp. Zool.* **250**, 244–252
23. Clark, J.J., Ilgen, T.L., Haire, M.F., and Mykles, D.L. (1991) Differential effects of oleic acid, sodium dodecyl sulfate, and protease inhibitors on the endopeptidase activities of the lobster multicatalytic proteinase. *Comp. Biochem. Physiol. B.* **99**, 413–417
24. Luckett, S., Garcia, R.S., Barker, J.J., Konarev, A.V., Shewry, P.R., Clarke, A.R., and Brady, R.L. (1999) High-resolution structure of a potent, cyclic proteinase inhibitor from sunflower seeds. *J. Mol. Biol.* **290**, 525–533
25. Hori, H., Nembai, T., Miyata, Y., Hayashi, T., Ueno, K., and Koide, T. (1999) Isolation and characterization of two 20S proteasomes from the endoplasmic reticulum of rat liver microsomes. *J. Biochem.* **126**, 722–730
26. Schagger, H. and von Jagow, G. (1987) Tricine-sodium dodecyl sulfate-polyacrylamide gel electrophoresis for the separation of proteins in the range from 1 to 100 kDa. *Anal. Biochem.* **166**, 368–379
27. Yamada, S., Hojo, K., Yoshimura, H., and Ishikawa, K. (1995) Reaction of 20S proteasome: shift of SDS-dependent activation profile by divalent cations. *J. Biochem.* **117**, 1162–1169
28. Otlewski, J., Polanowski, A., Leluk, J., and Wilusz, T. (1984) Trypsin inhibitors in summer squash (Cucurbita pepo) seeds. Isolation, purification and partial characterization of three inhibitors. *Acta. Biochim. Pol.* **31**, 267–278
29. Kress, L.F. and Laskowski, M., Sr. (1967) The basic trypsin inhibitor of bovine pancreas. VII. Reduction with borohydride of disulfide bond linking half-cystine residues 14 and 38. *J. Biol. Chem.* **242**, 4925–4929
30. Liu, W.K. and Meienhofer, J. (1968) Preparation of 14,38-bis-[S-carbamidomethyl]-(basic trypsin inhibitor) possessing full biological activity. *Biochem. Biophys. Res. Commun.* **31**, 467–473
31. Goldenberg, D.P. (1988) Kinetic analysis of the folding and unfolding of a mutant form of bovine pancreatic trypsin inhibitor lacking the cysteine-14 and -38 thiols. *Biochemistry* **27**, 2481–2489
32. Marks, C.B., Naderi, H., Kosen, P.A., Kuntz, I.D., and Anderson, S. (1987) Mutants of bovine pancreatic trypsin inhibitor lacking cysteines 14 and 38 can fold properly. *Science* **235**, 1370–1373
33. Klausner, R.D. and Sitia, R. (1990) Protein degradation in the endoplasmic reticulum. *Cell* **62**, 611–614
34. Kopito, R.R. (1997) ER quality control: the cytoplasmic connection. *Cell* **88**, 427–430
35. Hosokawa, N., Tremblay, L.O., You, Z., Herscovics, A., Wada, I., and Nagata, K. (2003) Enhancement of endoplasmic reticulum (ER) degradation of misfolded Null Hong Kong alpha1-antitrypsin by human ER mannosidase I. *J. Biol. Chem.* **278**, 26287–26294
36. Hortin, G.L. and Murthy, J. (2002) Substrate size selectivity of 20S proteasomes: analysis with variable-sized synthetic substrates. *J. Protein. Chem.* **21**, 333–337
37. Otlewski, J. and Wilusz, T. (1985) The serine proteinase inhibitor from summer squash (Cucurbita pepo): some structural features, stability and proteolytic degradation. *Acta. Biochim. Pol.* **32**, 285–293
38. McCutchen-Maloney, S.L., Matsuda, K., Shimbara, N., Binns, D.D., Tanaka, K., Slaughter, C.A., and DeMartino, G N. (2000) cDNA cloning, expression, and functional characterization of PI31, a proline-rich inhibitor of the proteasome. *J. Biol. Chem.* **275**, 18557–18565
39. Bao, J., Sato, K., Li, M., Gao, Y., Abid, R., Aird, W., Simons, M., and Post, M.J. (2001) PR-39 and PR-11 peptides inhibit ischemia-reperfusion injury by blocking proteasome-mediated I kappa B alpha degradation. *Am. J. Physiol. Heart Circ. Physiol.* **281**, H2612–H2618
40. Kress, L.F., Wilson, K.A., and Laskowski, M., Sr. (1968) The basic trypsin inhibitor of bovine pancreas, Part 8. Changes in activity following substitution of reduced half-cystin res4ues 14 and 38 with sulfhydryl reagents. *J. Biol. Chem.* **243**, 1758–1762
41. Forster, A., Whitby, F.G., and Hill, C.P. (2003) The pore of activated 20S proteasomes has an ordered 7-fold symmetric conformation. *EMBO J.* **22**, 4356–4364
42. Kossiakoff, A.A., Randal, M., Guenot, J., and Eigenbrot, C. (1992) Variability of conformations at crystal contacts in BPTI represent true low-energy structures: correspondence among lattice packing and molecular dynamics structures. *Proteins* **14**, 65–74
43. Furuike, S., Hirokawa, J., Yamada, S., and Yamazaki, M. (2003) Atomic force microscopy studies of interaction of the 20S proteasome with supported lipid bilayers. *Biochim. Biophys. Acta.* **1615**, 1–6
44. Nagasawa, K., Higashi, T., Hosokawa, N., Kaufman, R.J., and Nagata, K. (2007) Simultaneous induction of the four subunits of the TRAP complex by ER stress accelerates ER degradation. *EMBO Rep.* **8**, 483–489
45. Meng, L., Mohan, R., Kwok, B.H.B., Elofsson, M., Sin, N., and Crews, C.M. (1999) Epoxomicin, a potent and selective proteasome inhibitor, exhibits in vivo antiinflammatory activity. *Proc. Natl. Acad. Sci. USA* **96**, 10403–10408
46. Braun, H.A., Umbreen, S., Groll, M., Kuckelkorn, U., Mlynarczuk, I., Wigand, M.E., Drung, I., Kloetzel, P.M., and Schmidt, B. (2005) Tripeptide mimetics inhibit the 20S proteasome by covalent bonding to the active site threonines. *J. Biol. Chem.* **280**, 28394–28401
47. Sharon, M., Witt, S., Felderer, K., Rockel, B., Baumeister, W., and Robinson, C.V. (2006) 20S proteasomes have the potential to keep substrates in store for continual degradation. *J. Biol. Chem.* **281**, 9569–9575
48. Huffman, H.A., Sadeghi, M., Seemuller, E., Baumeister, W., and Dunn, M.F. (2003) Proteasome-cytochrome c interactions: a model system for investigation of proteasome host-guest interactions. *Biochemistry* **42**, 8679–8686